National Technical University of Athens

Shallow water bathymetry from active and passive UAV-borne, airborne and satellite-borne remote sensing

Dr. Eng. Panagiotis Agrafiotis

http://users.ntua.gr/pagraf/

https://3deepvision.eu/

NTUA PHOTOGRAMMETRIC COMPUTER VISION

3[Deep]Vision Research Group

Seabed mapping for shallow waters

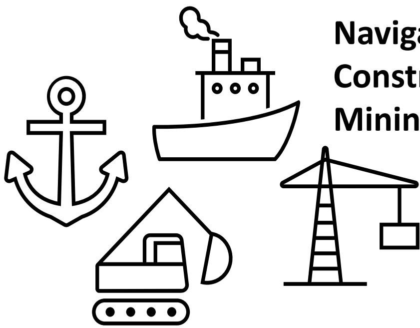

Navigation
Constructions
Mining

Touris
m

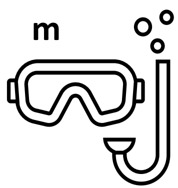

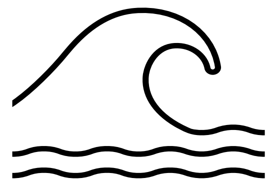

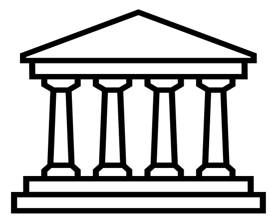

Marine litter
detection

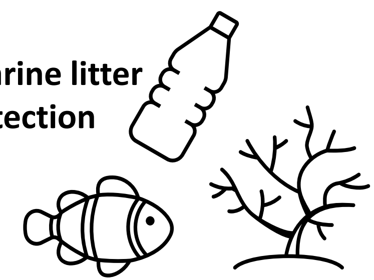

Marine animal
forests

Cultural Heritage

Agrafiotis: Bathymetry from active and passive UAV-borne, airborne and satellite-borne remote sensing

Shallow waters examples: Limassol marina, Cyprus

Shallow waters examples: Latsi, Cyprus

Shallow waters examples: Agia Napa, Cyprus

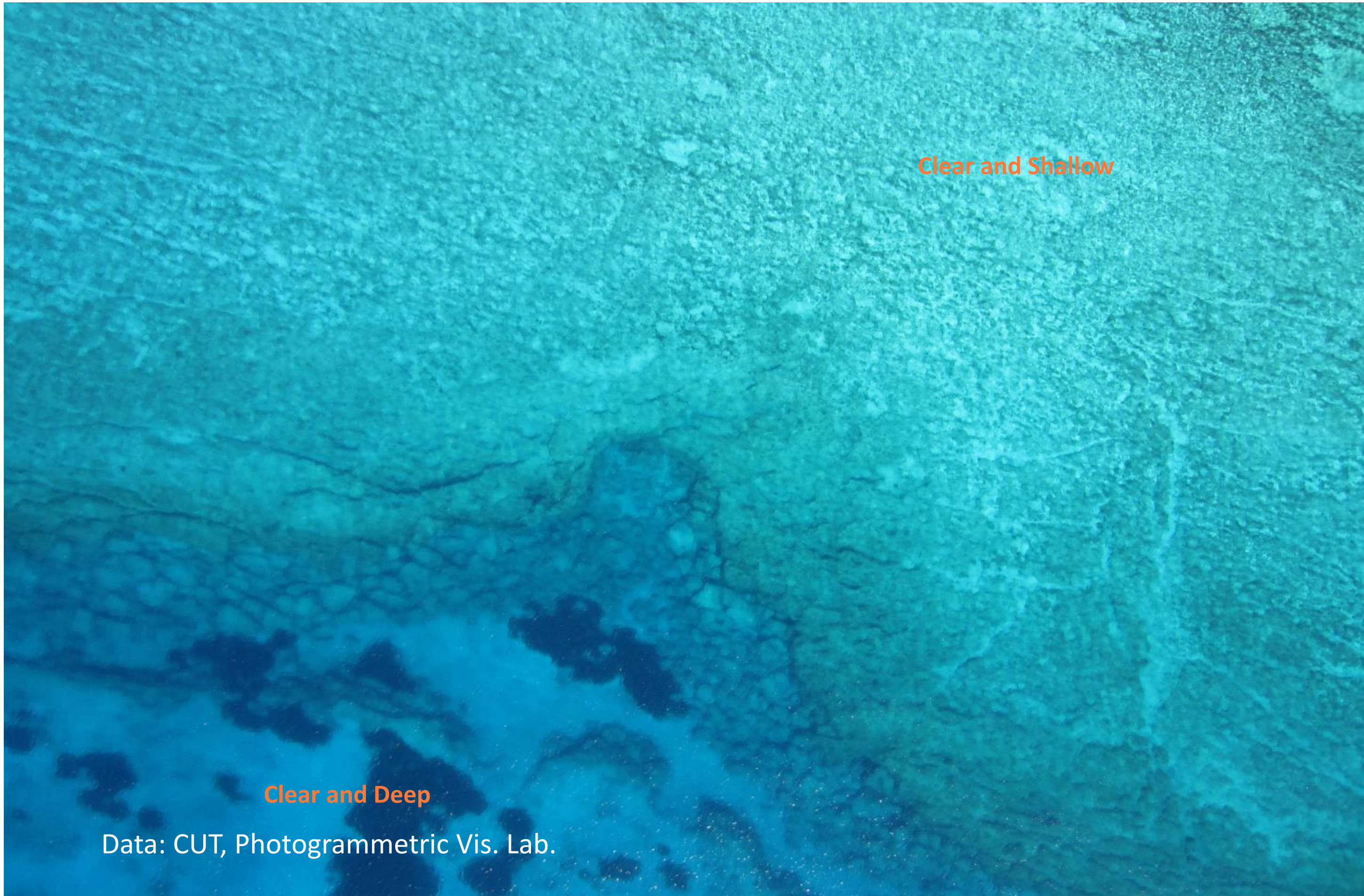

Shallow waters examples: Lemnos island, Greece

Shallow waters examples: Andros island, Bahamas

Shallow waters examples: Wadden Sea, Netherlands-Germany

Shallow waters examples: Ionian Sea, Greece

Bathymetry via active and passive airborne remote sensing

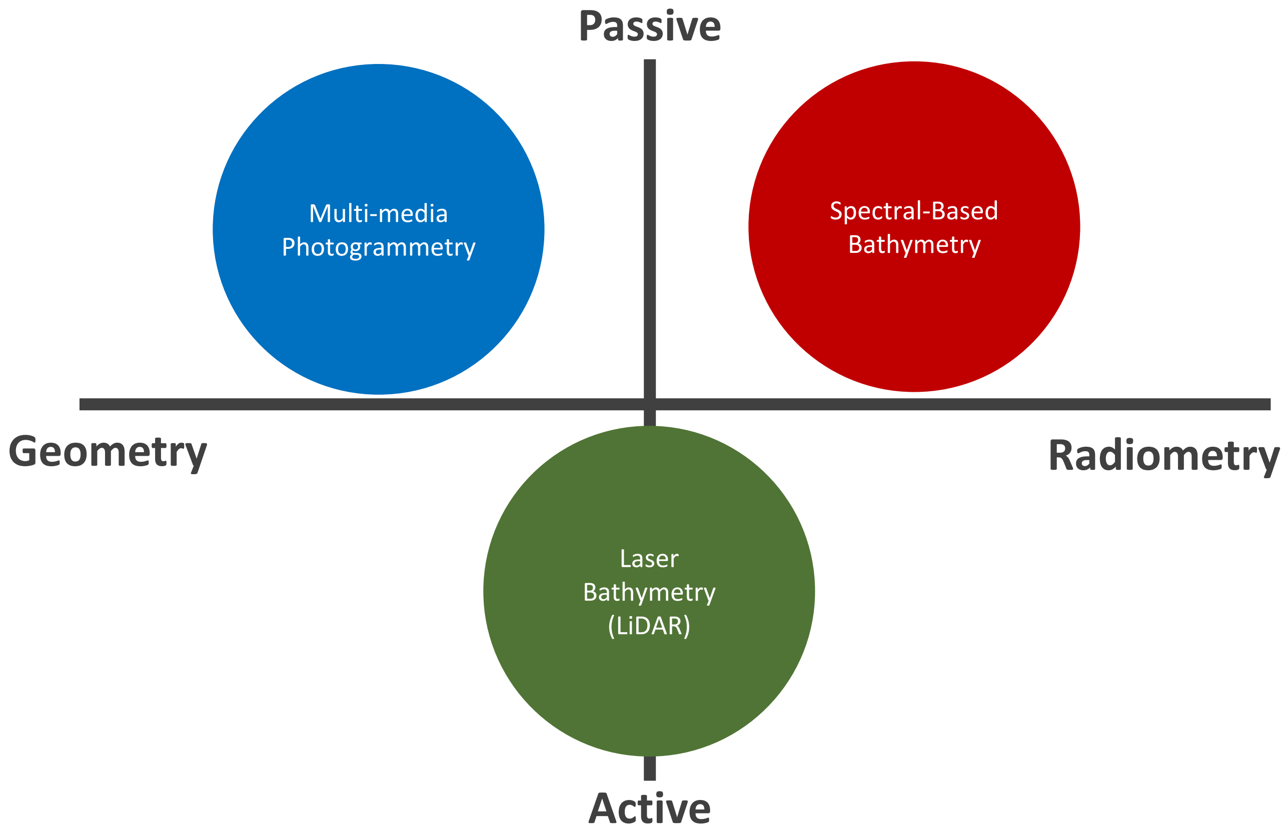

Agrafiotis: Bathymetry from active and passive UAV-borne, airborne and satellite-borne remote sensing

Colour loss – light absorption

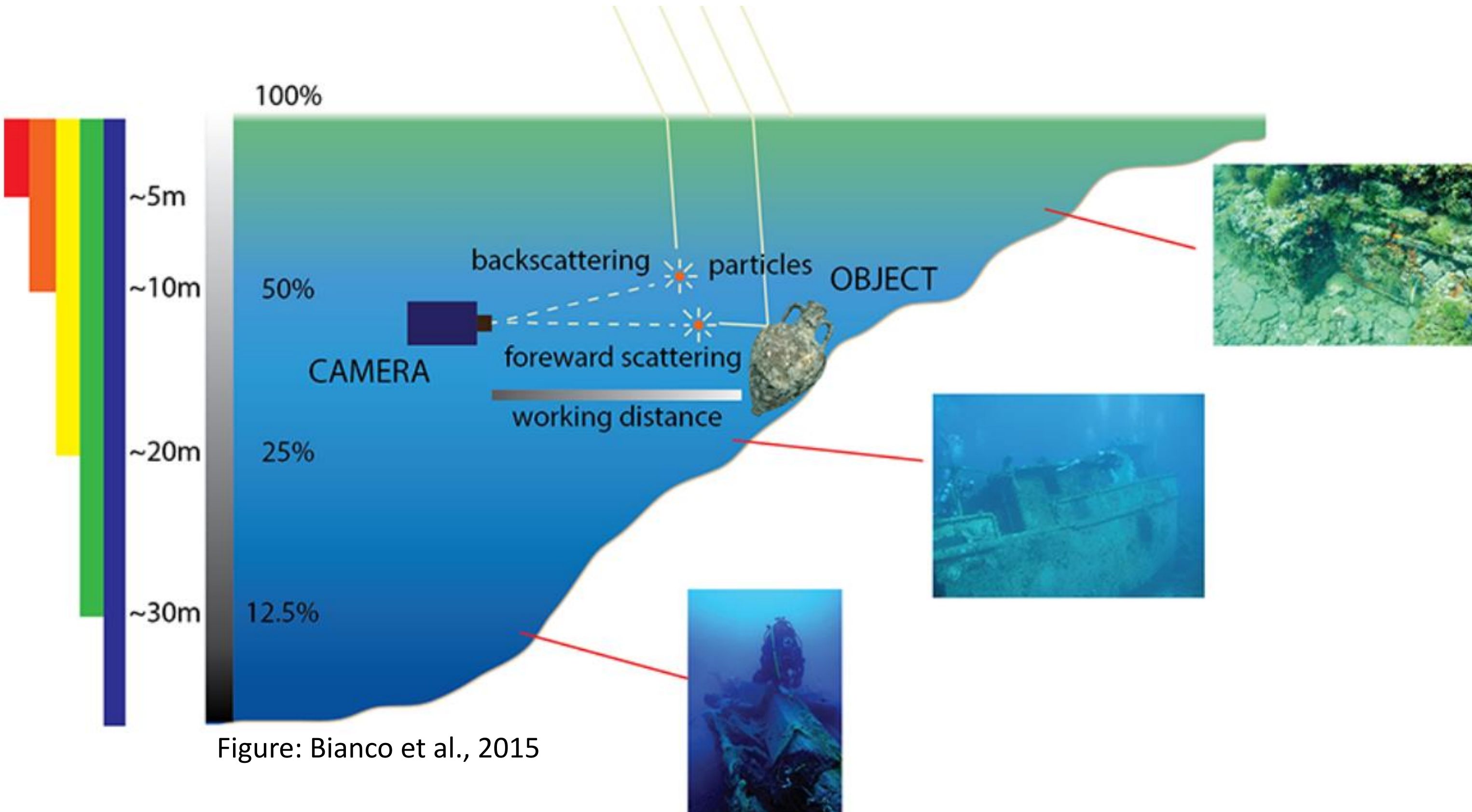

Figure: Bianco et al., 2015

Refraction effect

Snell's law

Snell's law states that the ratio of the sines of the angles of incidence and refraction is equivalent to the ratio of phase velocities in the two media, or equivalent to the reciprocal of the ratio of the indices of refraction.

$$\frac{\sin \theta_2}{\sin \theta_1} = \frac{v_2}{v_1} = \frac{n_1}{n_2}$$

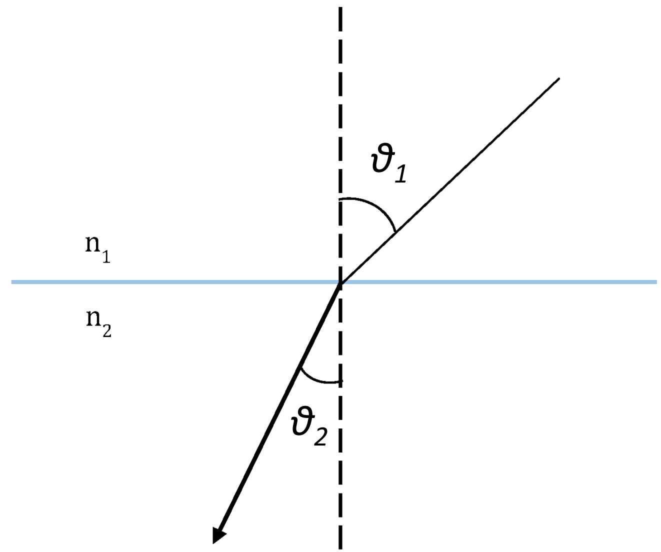

The law is based on **Fermat's principle**, also known as the principle of least time.

Fermat's principle states that the path taken by a ray between two given points is the path that can be traversed in the least time.

Airborne Laser Bathymetry - Geometry

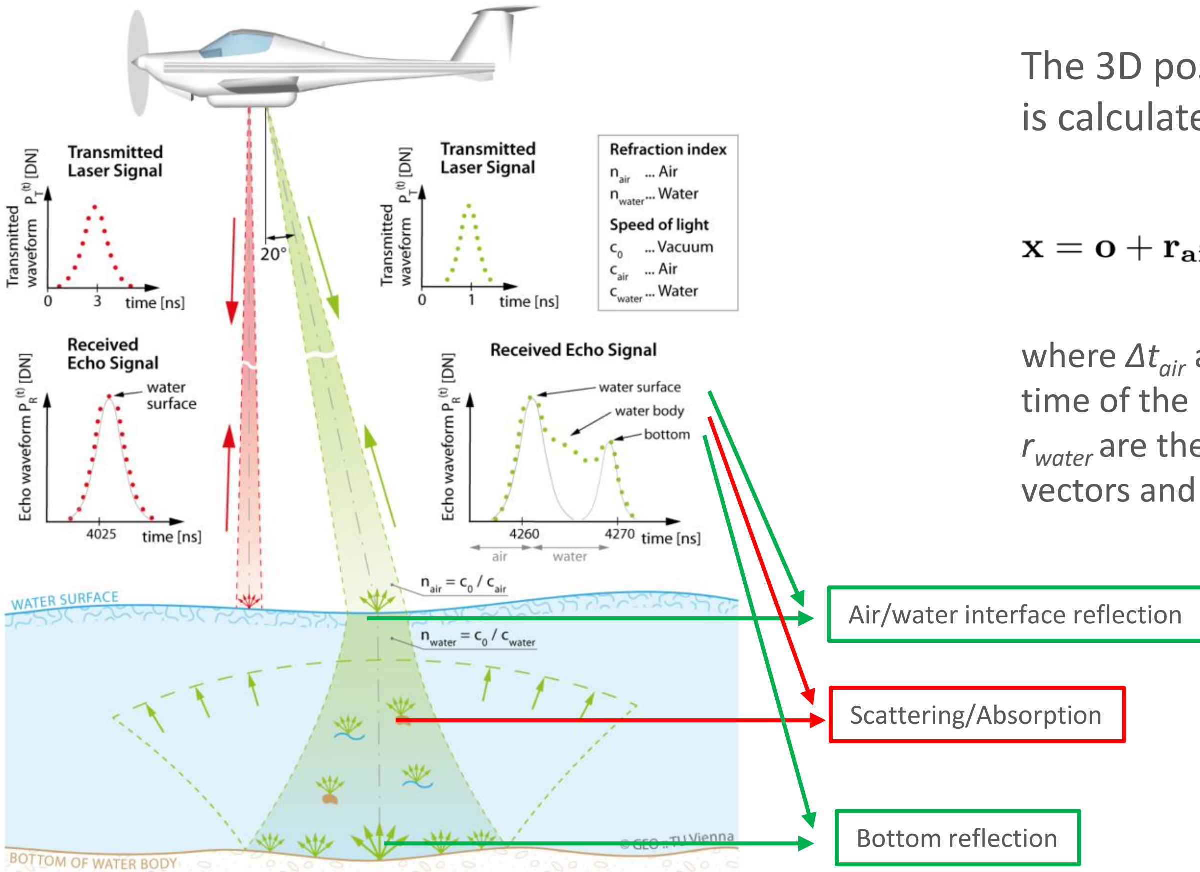

Figure: Mandlburger et al., 2013.

The 3D position x of a water bottom point is calculated by:

$$\mathbf{x} = \mathbf{o} + \mathbf{r_{air}} \frac{\Delta t_{air} c_{air}}{2} + \mathbf{r_{water}} \frac{\Delta t_{water} c_{water}}{2}$$

where Δt_{air} and Δt_{water} correspond to the round-trip time of the laser beam in air and water, r_{air} and r_{water} are the corresponding beam direction unit vectors and o is the scanner origin.

Multi-media Photogrammetry – Single View Geometry

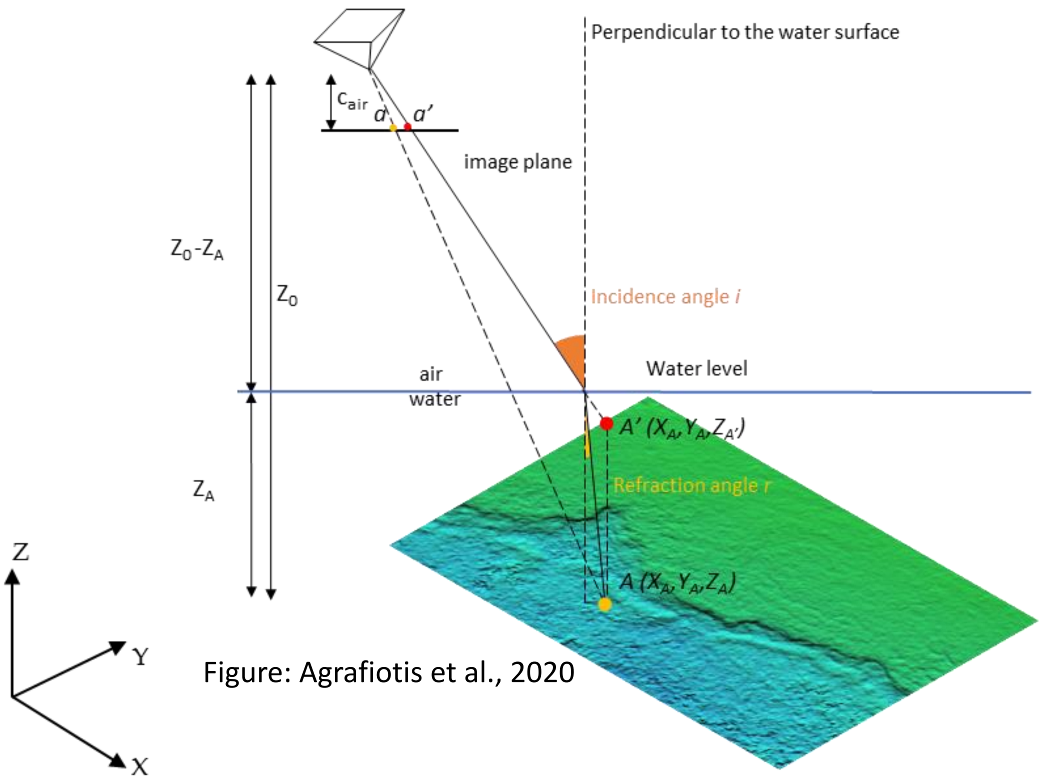

Figure: Agrafiotis et al., 2020

- Violation of the Collinearity Equation
- Apparent depths

Multi-media Photogrammetry – Multiple View Geometry

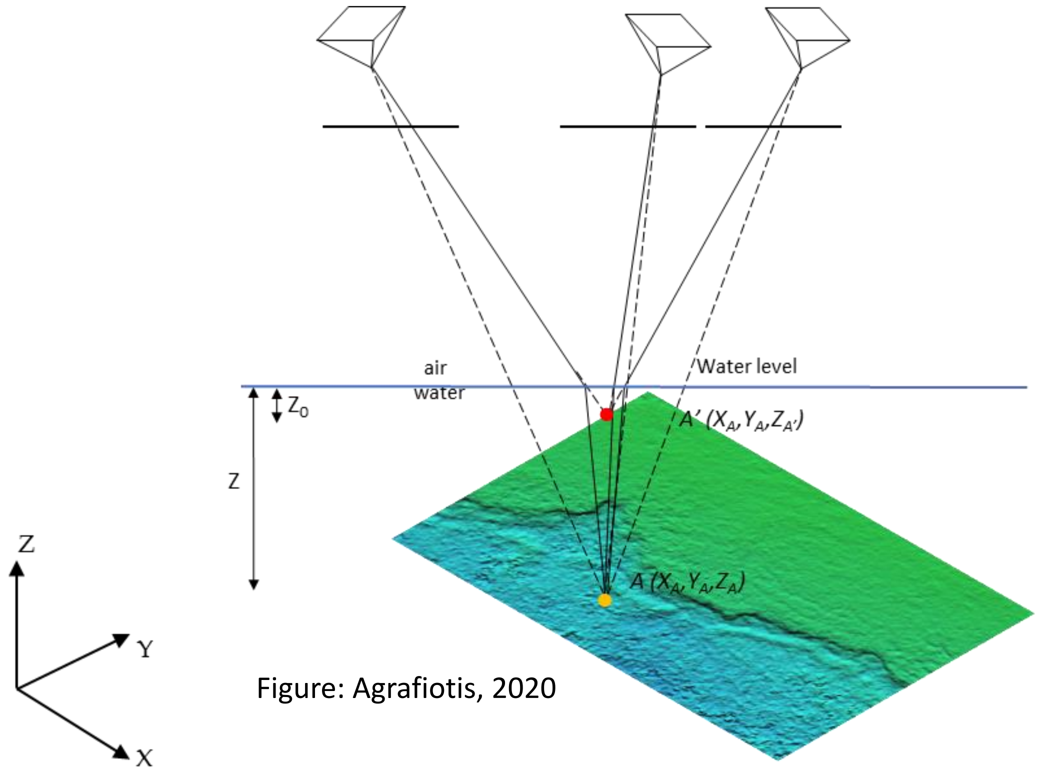

Figure: Agrafiotis, 2020

- Violation of the Collinearity Equation
- Apparent depths
- **Increased noise in the point clouds**

Multi-media Photogrammetry – Correction Basics

- **Analytical correction:** modification of the collinearity equation.
- **Image-space correction**: re-projection of the original photo to correct the water refraction.
- **Machine learning-based**: depends on machine learning models that learn the underestimation of depths and predict the correct depth knowing only the apparent one.

*Other methods: multiplying the apparent depth with a constant number, which in most of the cases is the refraction index of the water the use of this form of correction might be acceptable in the very shallow waters, however, **remarkable errors are expected after 2-3 m depth.***

Multi-media Photogrammetry – Image Space Correction

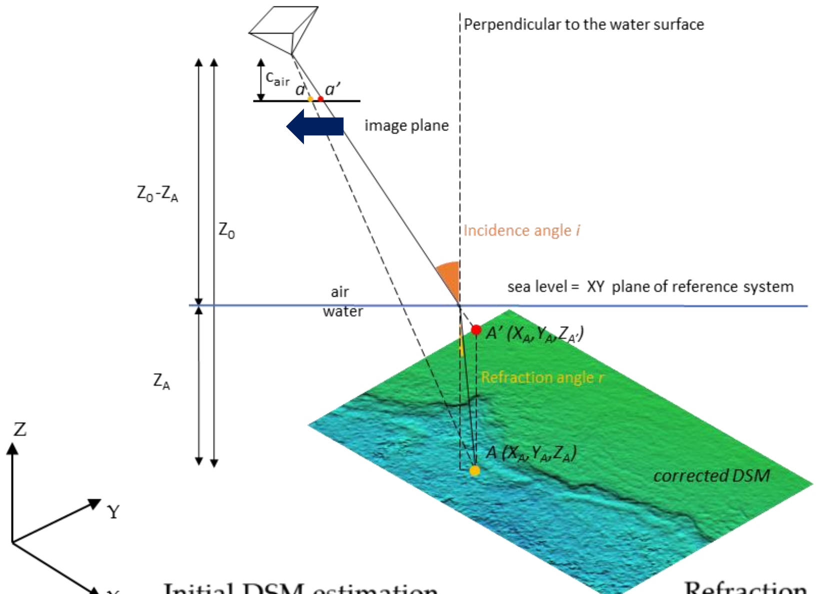

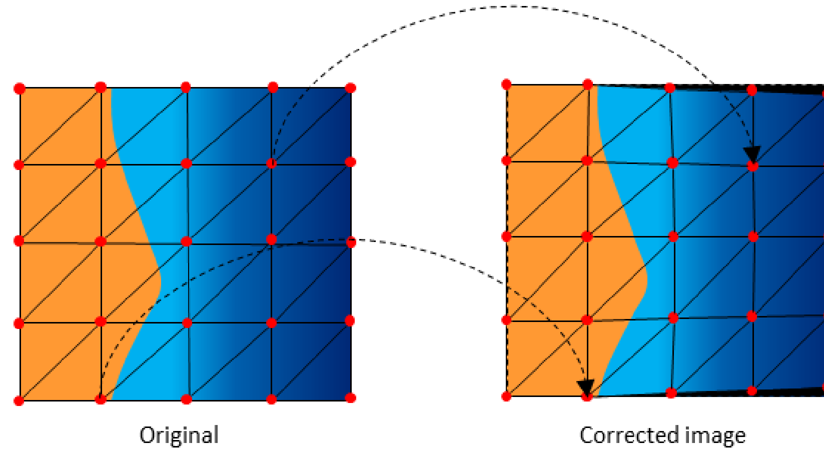

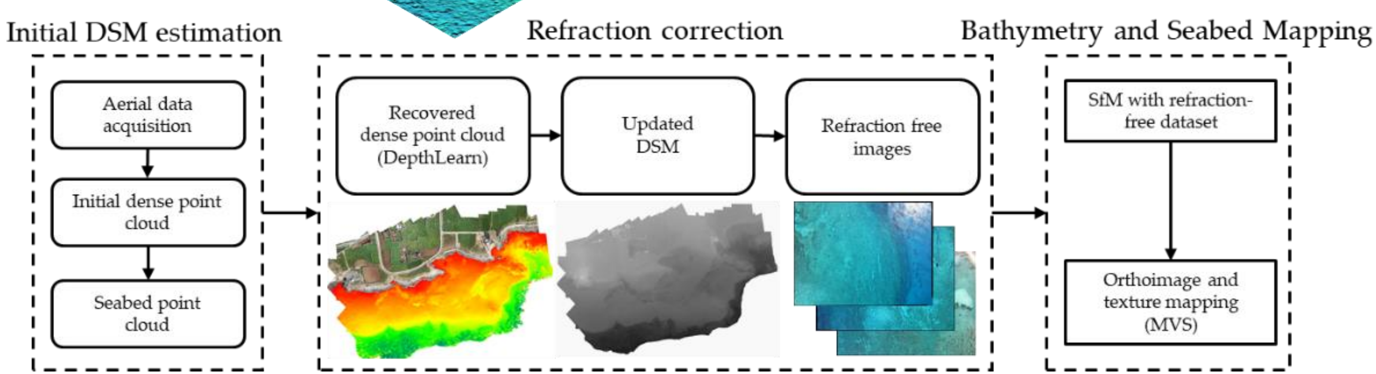

Figures: Agrafiotis et al., 2020

Multi-media Photogrammetry – ML-based Correction

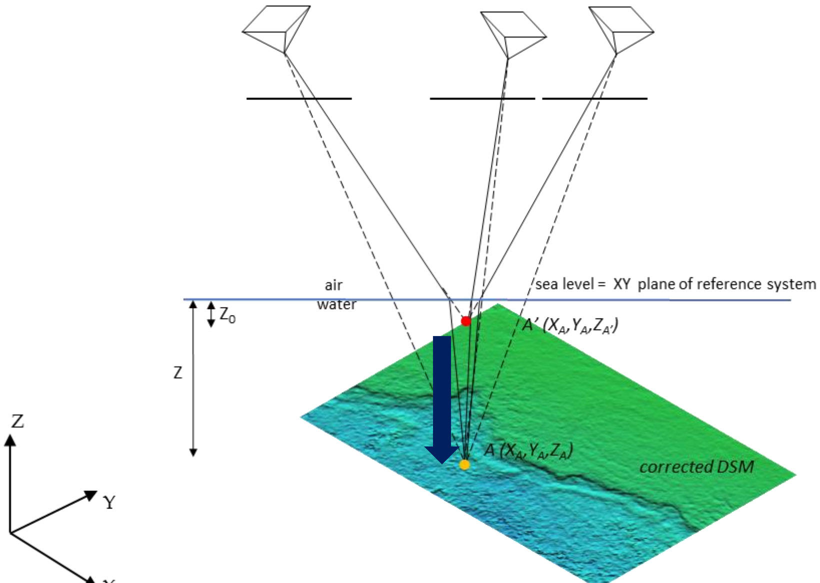

Agrafiotis et al., 2019: $f(Z_0) = \sum_{n=1}^{N} (a_n + \widehat{a}_n)\, k(Z_0,\, Z_{0n}) + b$

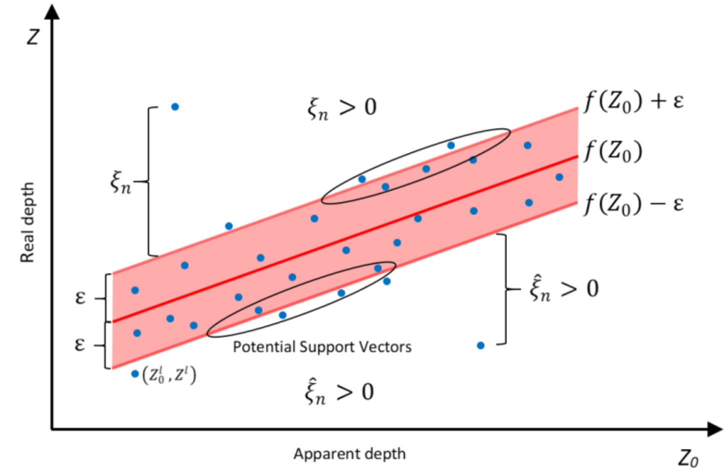

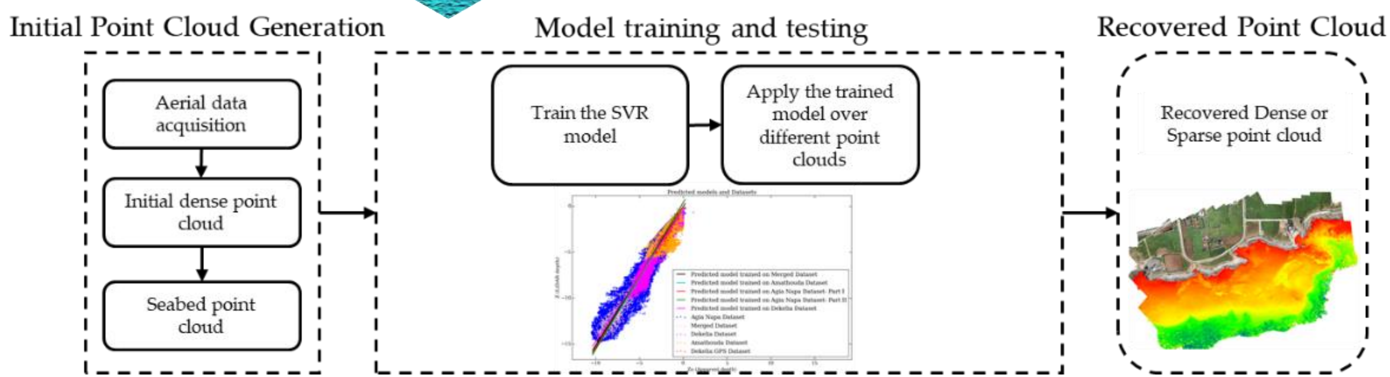

Figures: Agrafiotis et al., 2020

Spectral-based bathymetry

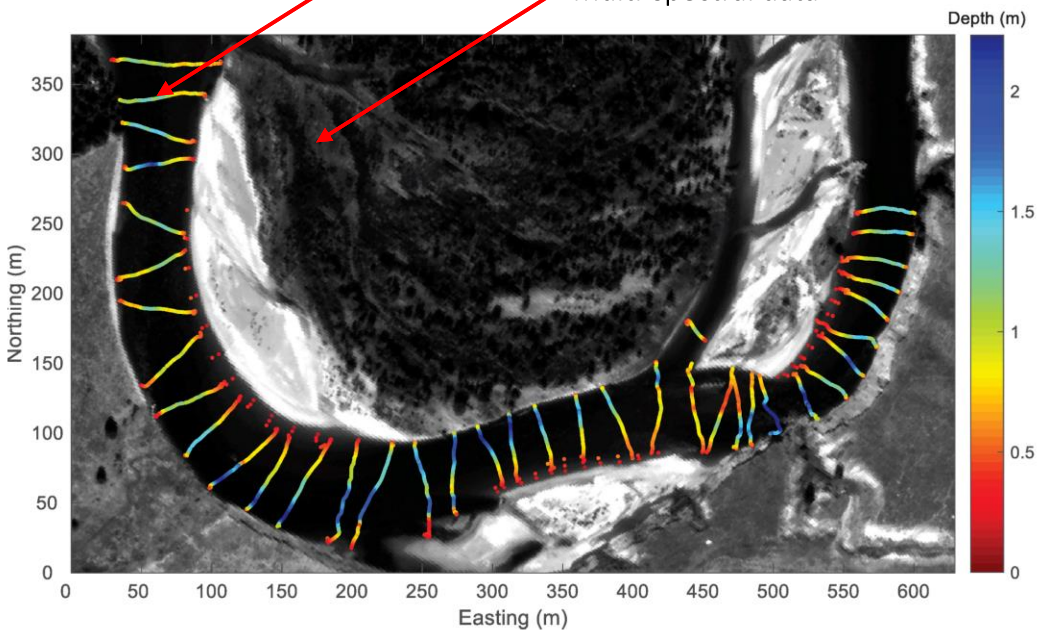

Figures: Legleiter et al., 2018,

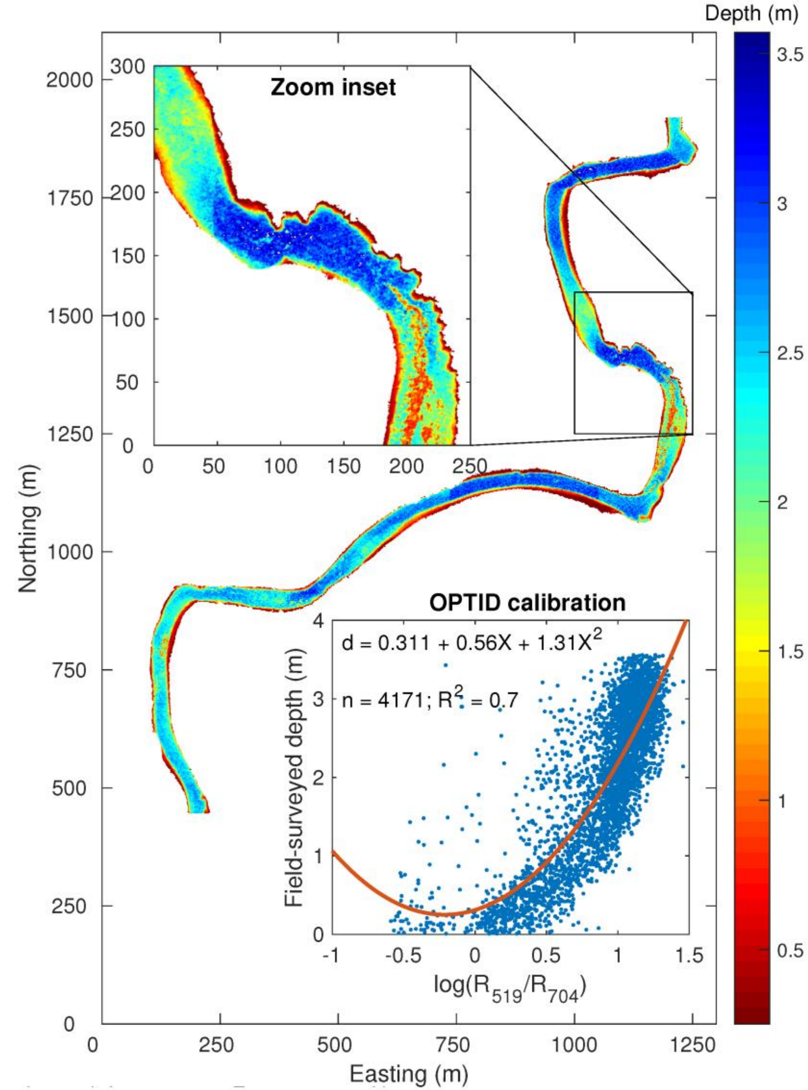

Basics of spectrally-based bathymetry

$$L_T(\lambda) = L_p(\lambda) + L_s(\lambda) + L_c(\lambda) + L_b(\lambda)$$

L_T is the total upwelling radiance
L_p are the contributions from the atmosphere
L_s is the radiance reflected from the water surface
L_c is the radiance from the water column
L_b is the bottom-reflected radiance

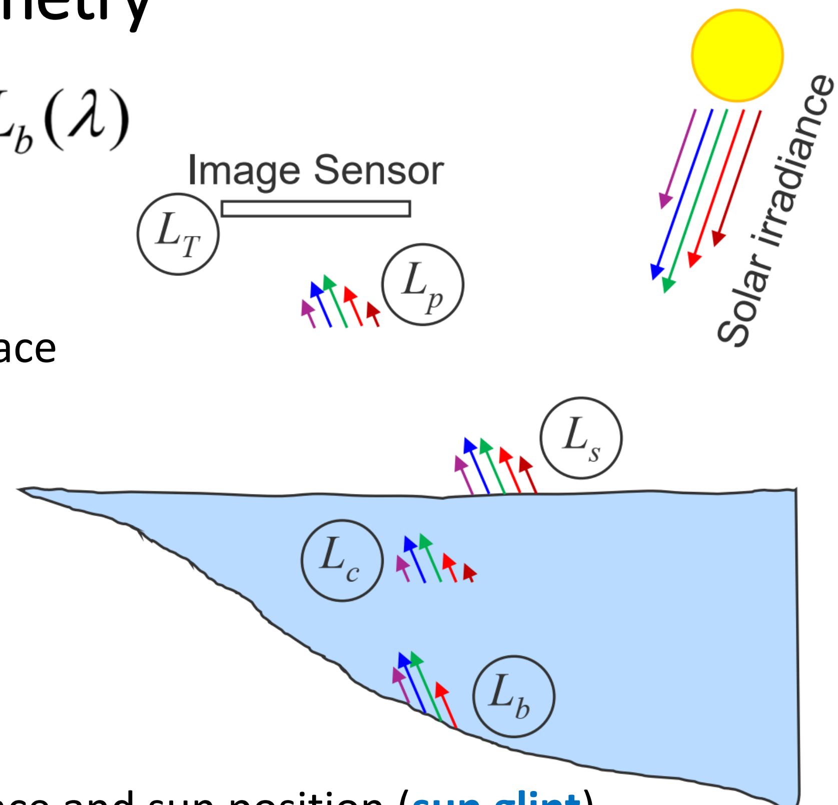

L_s depends on the roughness of the water surface and sun position (**sun glint**)
L_b is related to **depth** and is the radiance reflected by the **bottom**
L_c is related to the water's optical property (i.e. **turbidity**)

Slide retrieved from Mandlburger 2017, "Bathymetry from active and passive airborne remote sensing – looking back and ahead"

Common colour-to-depth relation/methodology

- The standard linear algorithm (Lyzenga, 1978) assumes a log-linear relationship between reflectance ($R(\lambda i)$) and water depth (z):

$$z = b \log R(\lambda_i) + c$$

- Stumpf et al., 2003 bathymetric algorithm
The method approximates "physics" of light in the water:

pSDB "pseudo depth"

$$Z = m_1 \frac{\ln(nR_w(\lambda_i))}{\ln(nR_w(\lambda_j))} - m_0$$

where m_1 is a tunable constant to scale the ratio to depth, n is a fixed constant for all areas, and m_0 is the offset for a depth of 0 m

- Empirically tune coefficients
- Tuning successful with chart soundings/LiDAR etc.
- Generalized model

- Cluster-Based Method (CBR)

- SVMs

Factors affecting Spectral-based bathymetry (UAV or SDB)

Sun glint • Turbidity • High Aerosol

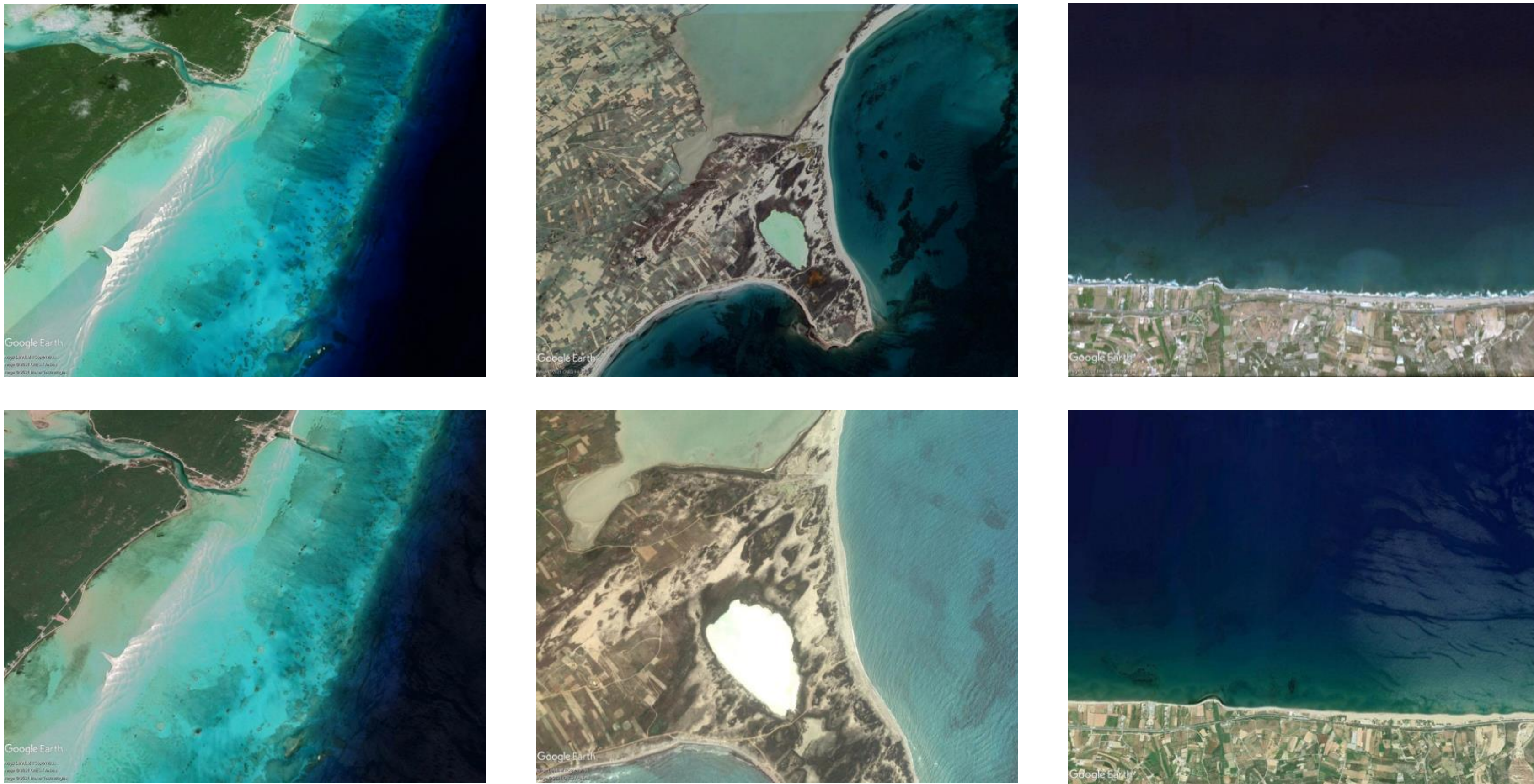

Images source: Google Earth

Factors affecting Spectral-based bathymetry (UAV or SDB)

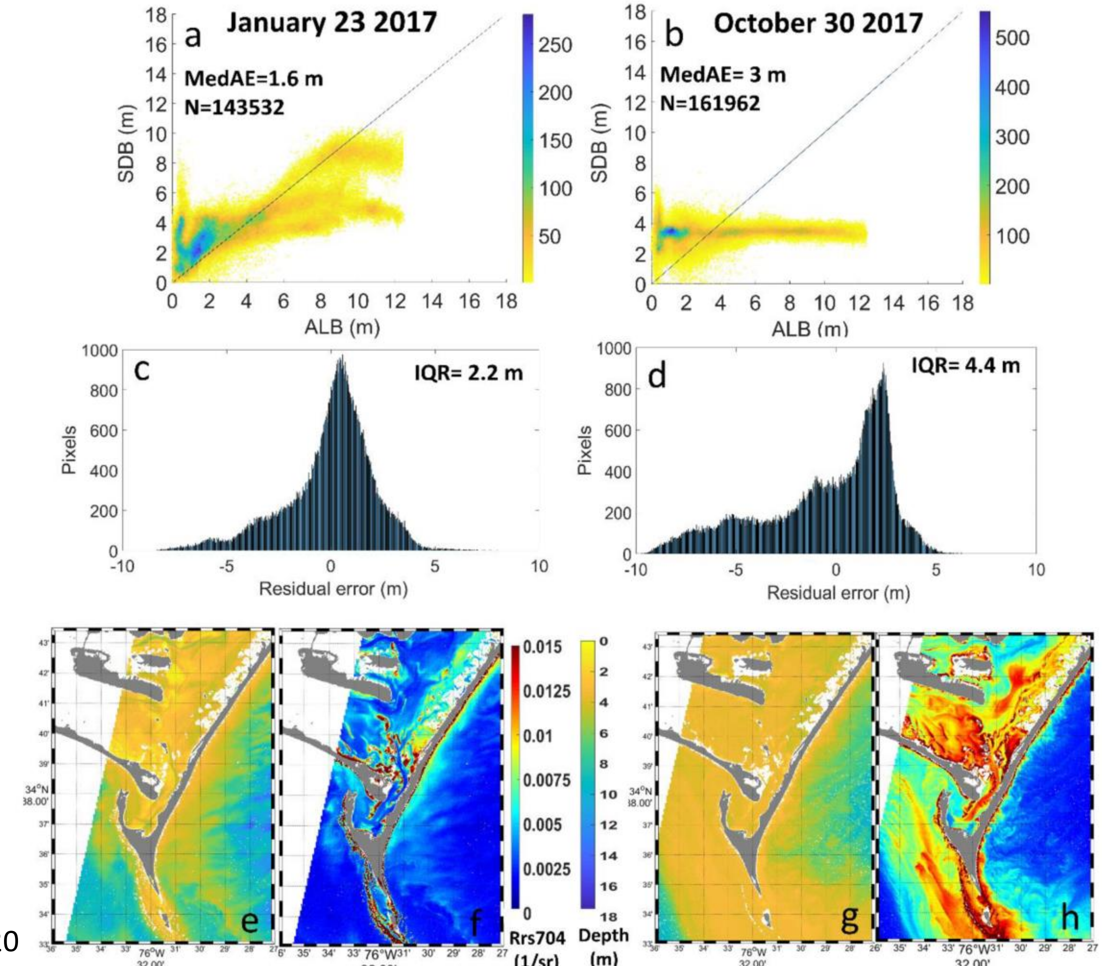

Figures: Caballero and Stumpf, 2020

Factors affecting Spectral-based bathymetry (UAV or SDB) - Solution

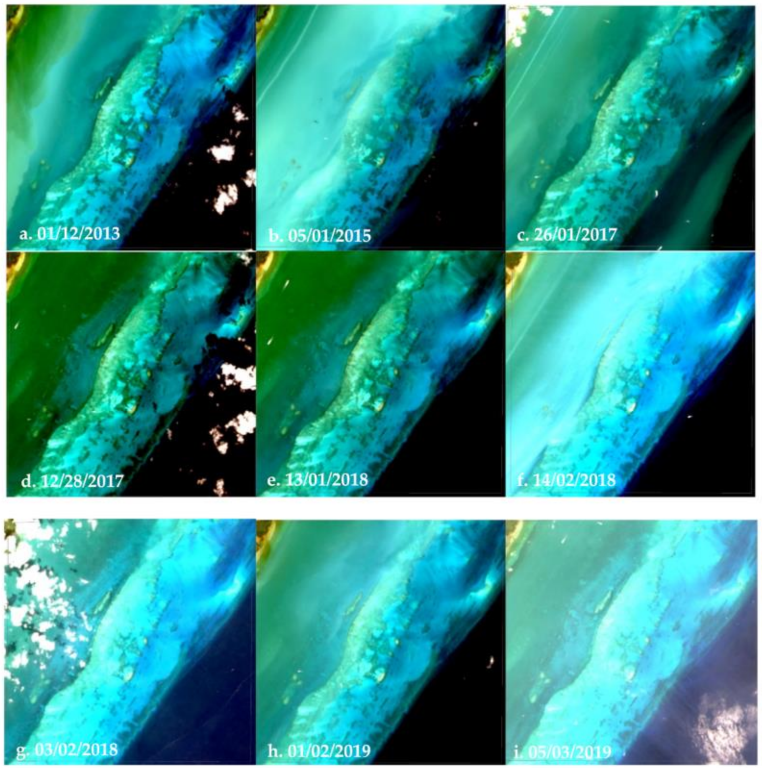

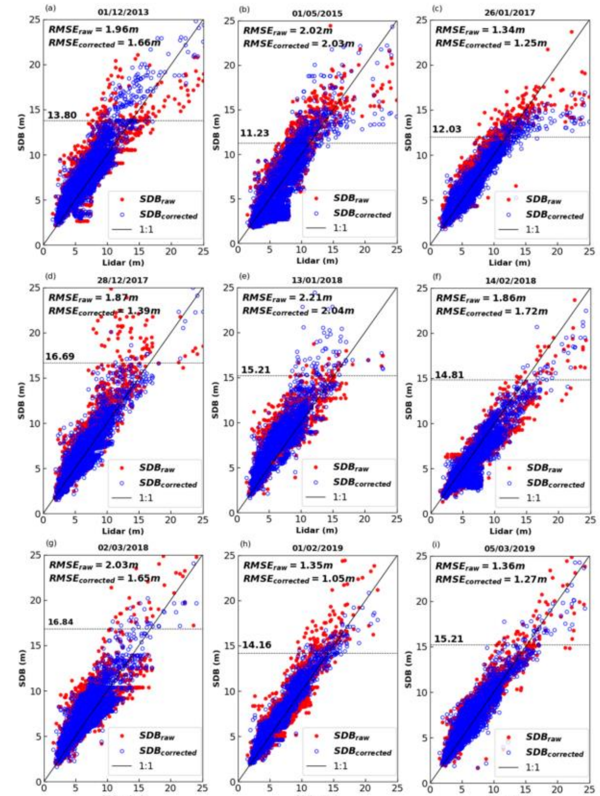

Figures: Ilori and Knudby, 2020

Physics-based multi-scene processing to improve the accuracy

Examples-Airborne Laser Bathymetry

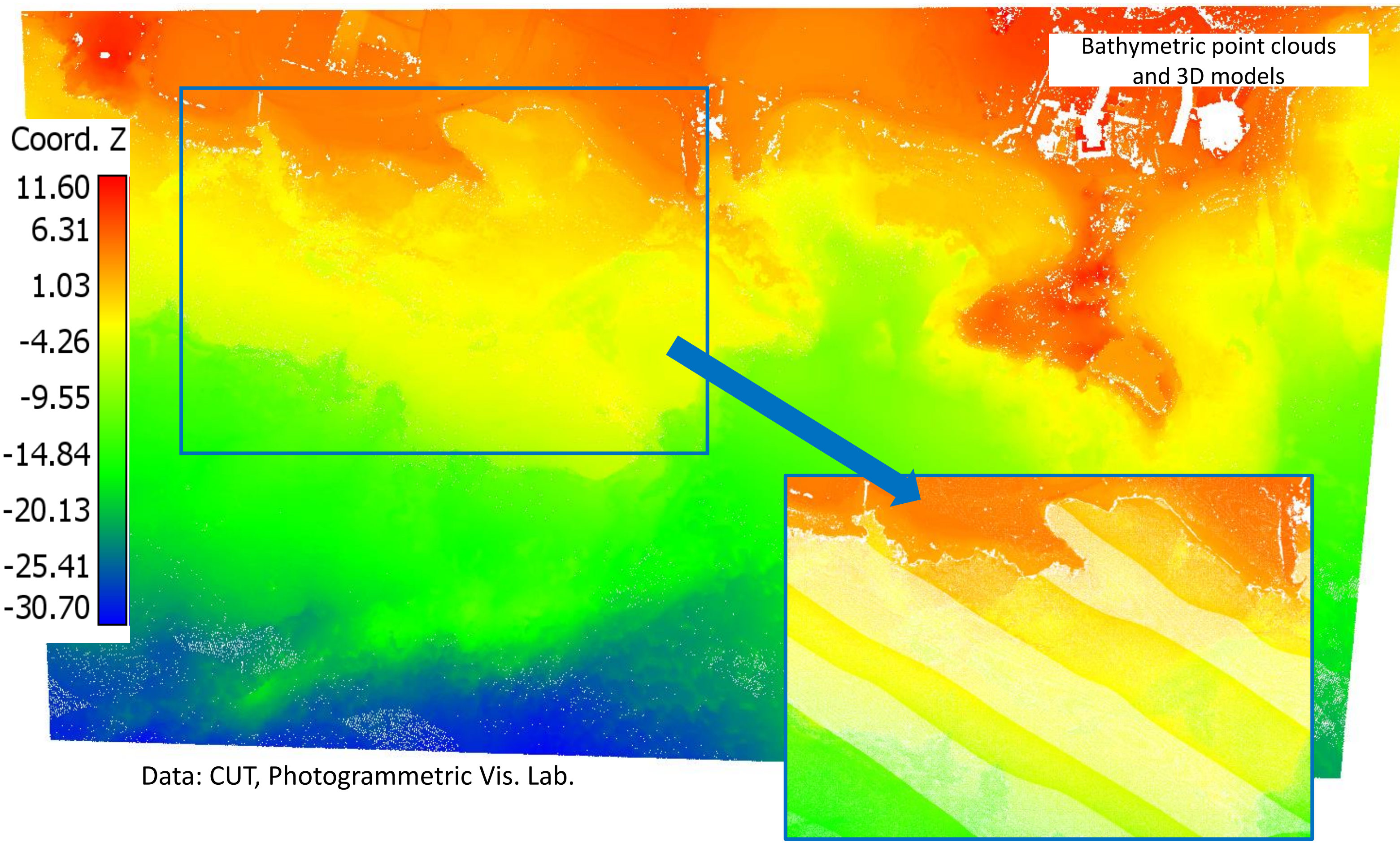

Data: CUT, Photogrammetric Vis. Lab.

Examples-Satellite-borne Laser Bathymetry

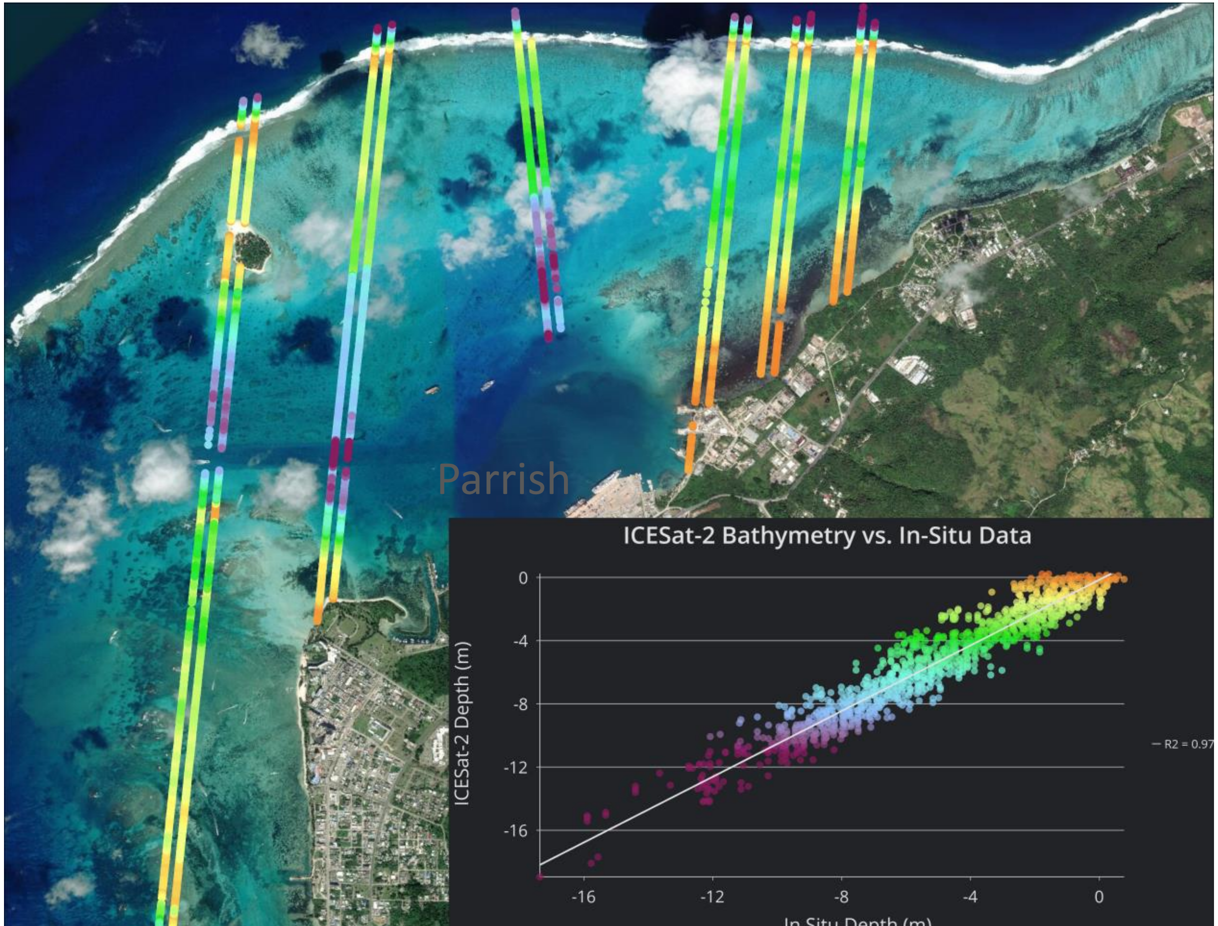

Figure: TCARTA, https://www.tcarta.com/events/geospatial-intelligence-month-april-2020

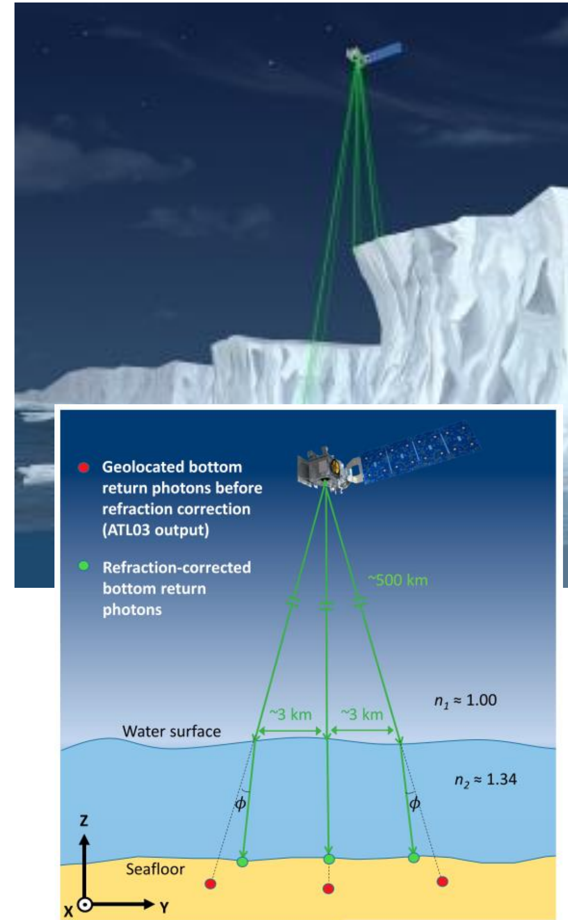

Figure: Parrish et al, 2019

Examples-Spectral-based Bathymetry – Satellite-borne

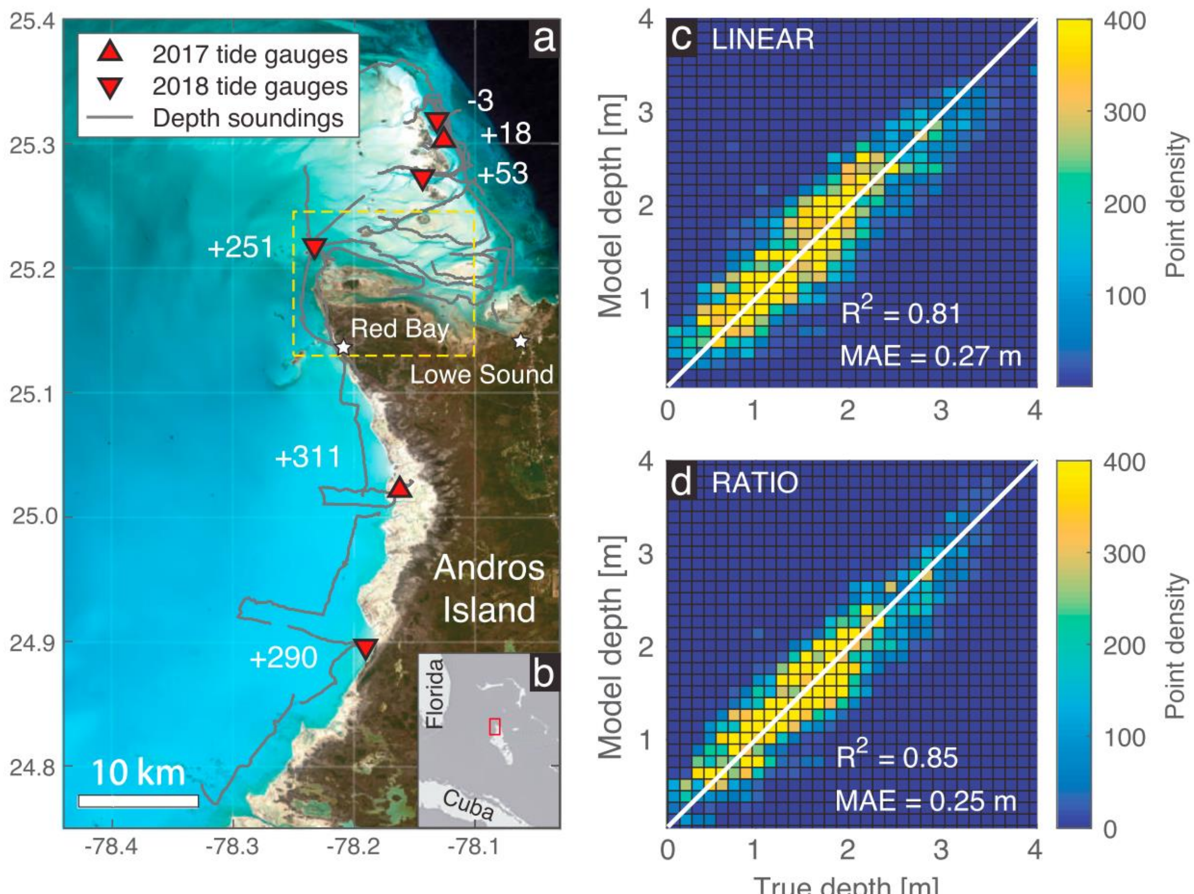

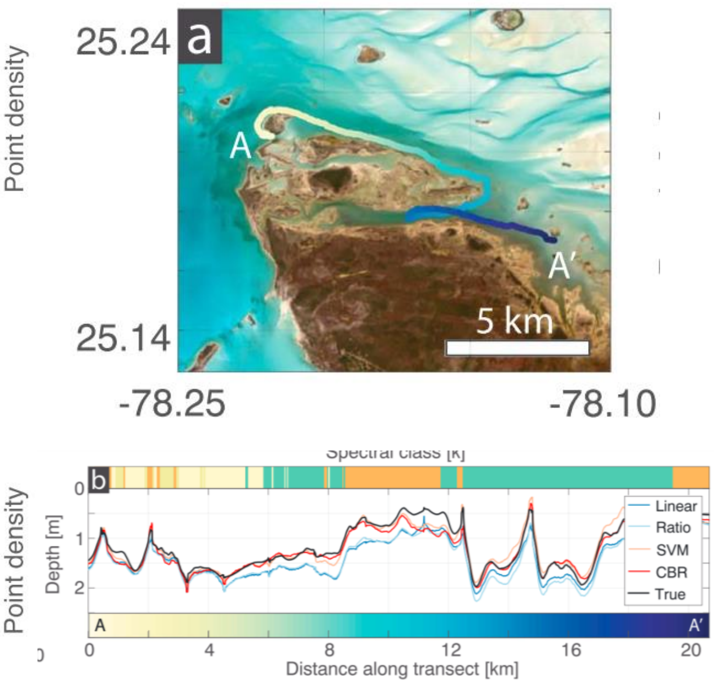

Figures: Geyman and Maloof, 2019

Examples-UAV-borne Multimedia Photogrammetry

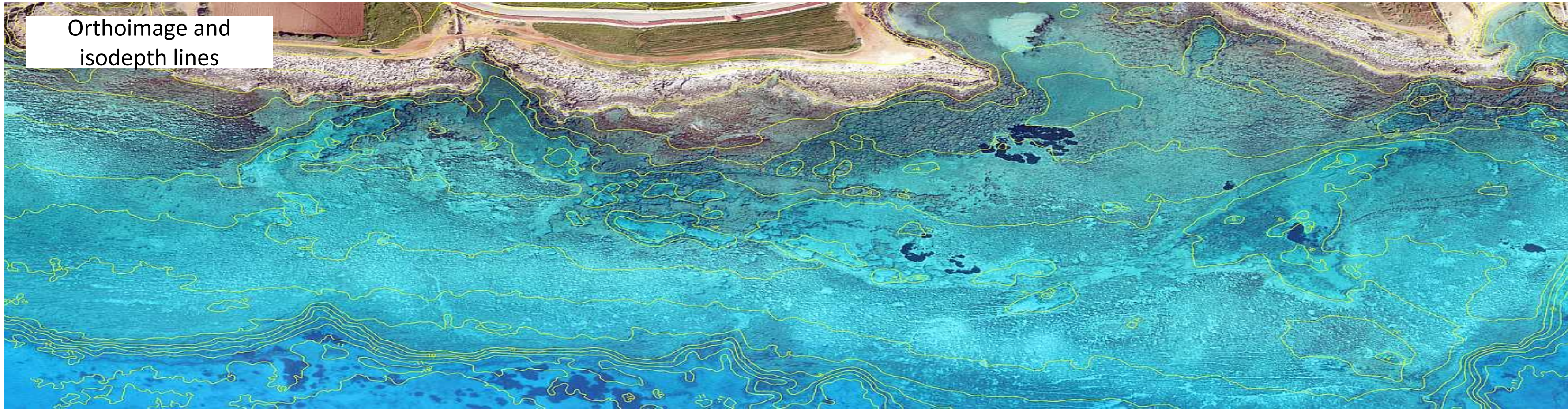

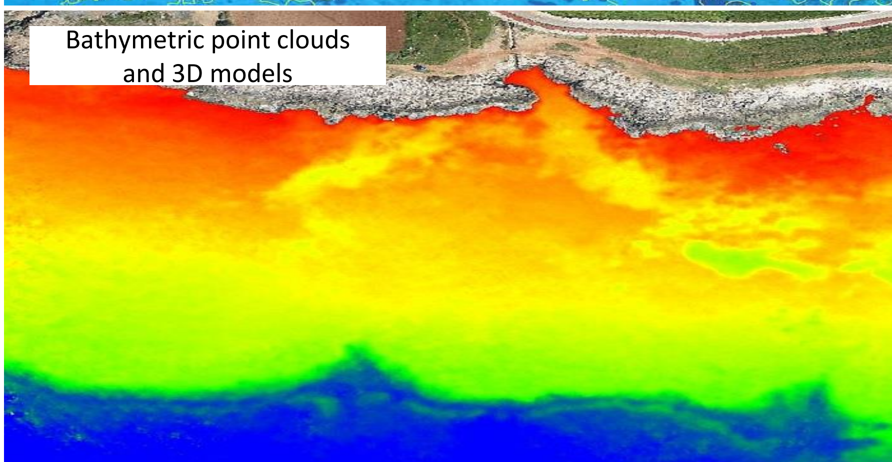

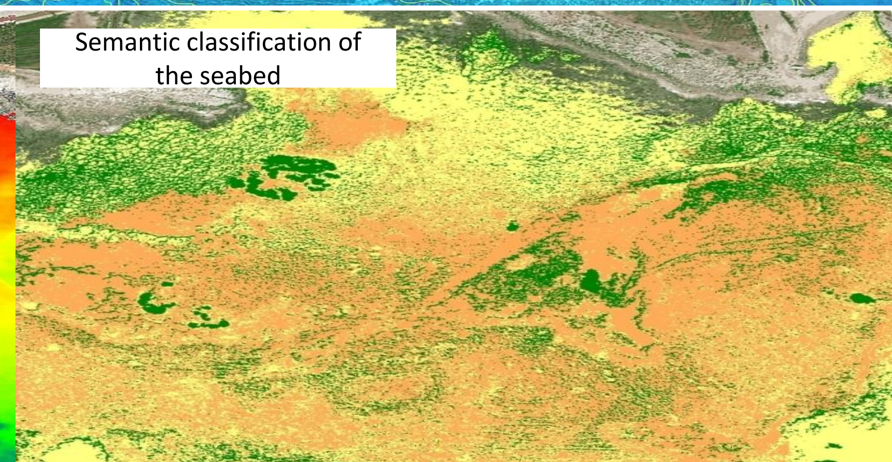

Data: CUT, Photogrammetric Vis. Lab., 3[Deep]Vision https://3deepvision.eu/

Examples-UAV-borne Multimedia Photogrammetry

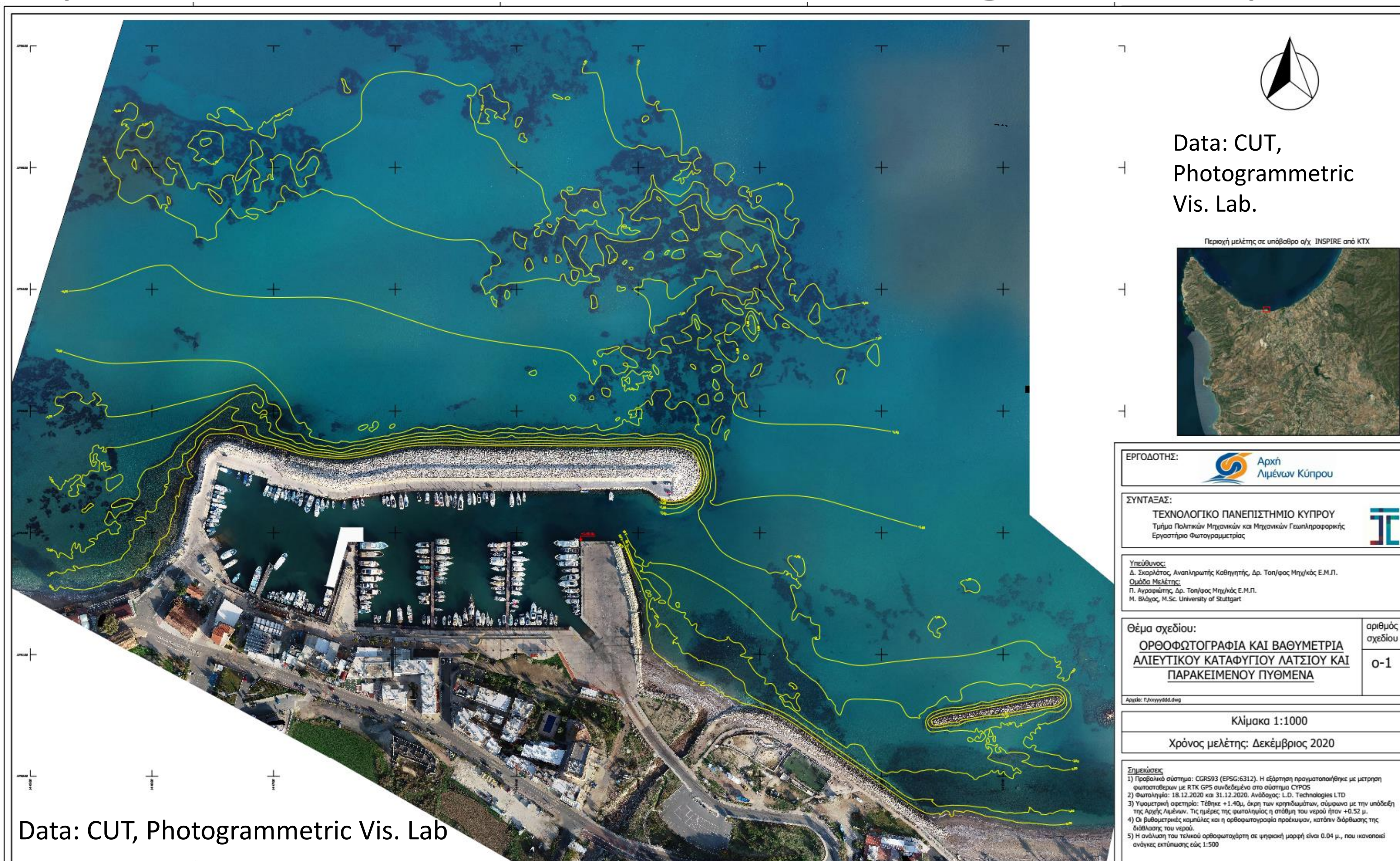

A deeper look into Multimedia Photogrammetry
Errors due to refraction

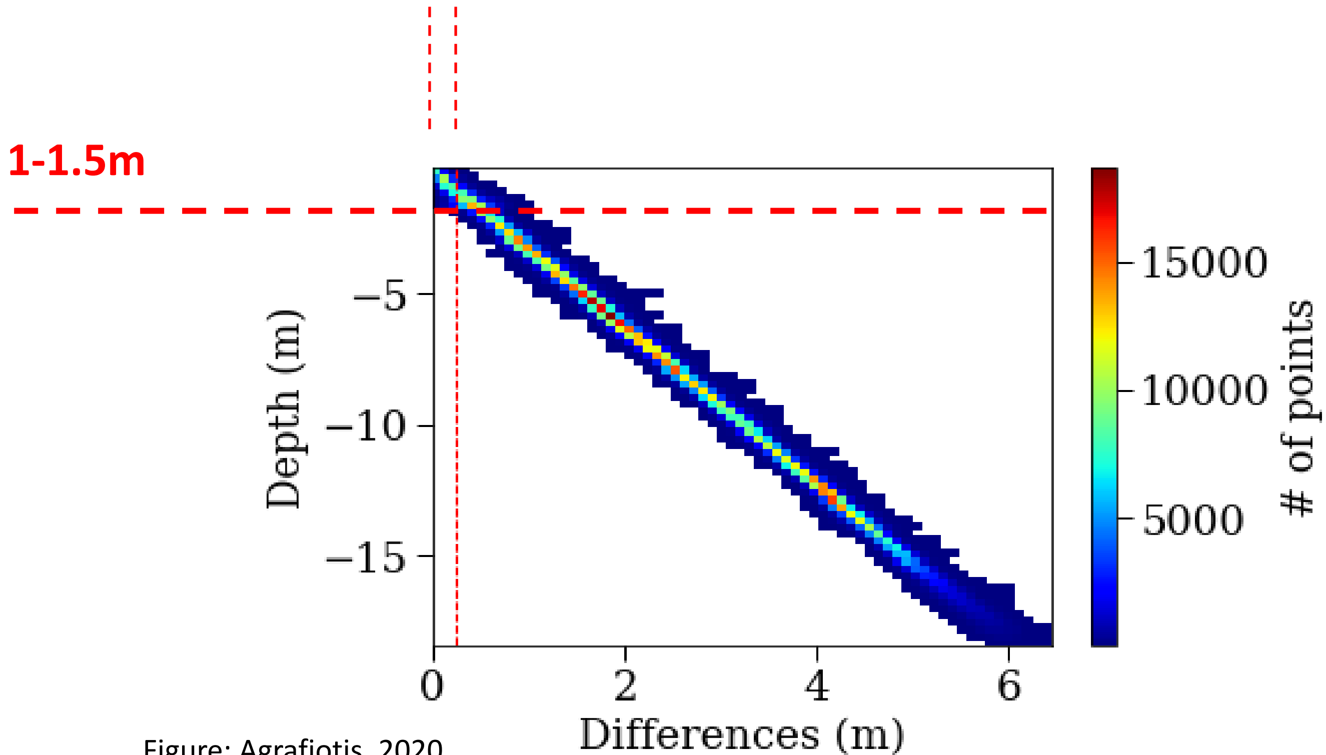

Figure: Agrafiotis, 2020

Ratio-based VS ML-based refraction correction methods

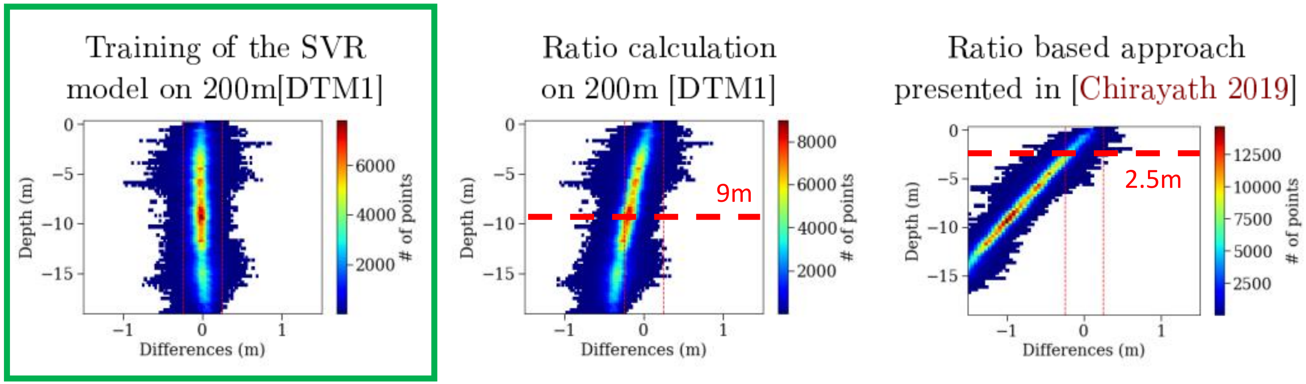

Dataset [training %]	Evaluation Site [testing %]	Max /Min depth of test site	Evaluation points	Uncorrected data			SVR corrected data			Ratio corrected data		
				$\bar{x}$ [m]	s [m]	$RMSE_Z$ [m]	$\bar{x}$ [m]	s [m]	$RMSE_Z$ [m]	$\bar{x}$ [m]	s [m]	$RMSE_Z$ [m]
150m [DTM1]	150m [DTM1]	18.7/0	2.461.488	2.48	1.47	2.874	**0.006**	**0.070**	**0.073**	-0.088	0.121	0.149
200m [DTM1]	200m [DTM1]	18.7/0	1.409.673	2.49	1.49	2.883	**0**	**0.109**	**0.109**	-0.108	0.164	0.197
200m [DTM2]	200m [DTM2]	19.05/0	2.097.713	2.96	1.54	3.337	**0.001**	**0.090**	**0.077**	-0.079	0.116	0.140
200m [DTM1]	200m [DTM2]	19.05/0	2.097.713	2.96	1.54	3.337	**-0.014**	**0.090**	**0.093**	-0.181	0.166	0.247
Cross site approach			Overall Average	2.643	1.500	3.031	**-0.002**	**0.090**	**0.088**	-0.114	0.142	0.183
			s	0.224	0.029	0.216	**0.009**	**0.016**	**0.016**	0.046	0.027	0.049

Figures and Table: Agrafiotis, 2020

Errors in the orthoimages due to refraction

Uncorrected | Corrected | Uncorrected | Corrected

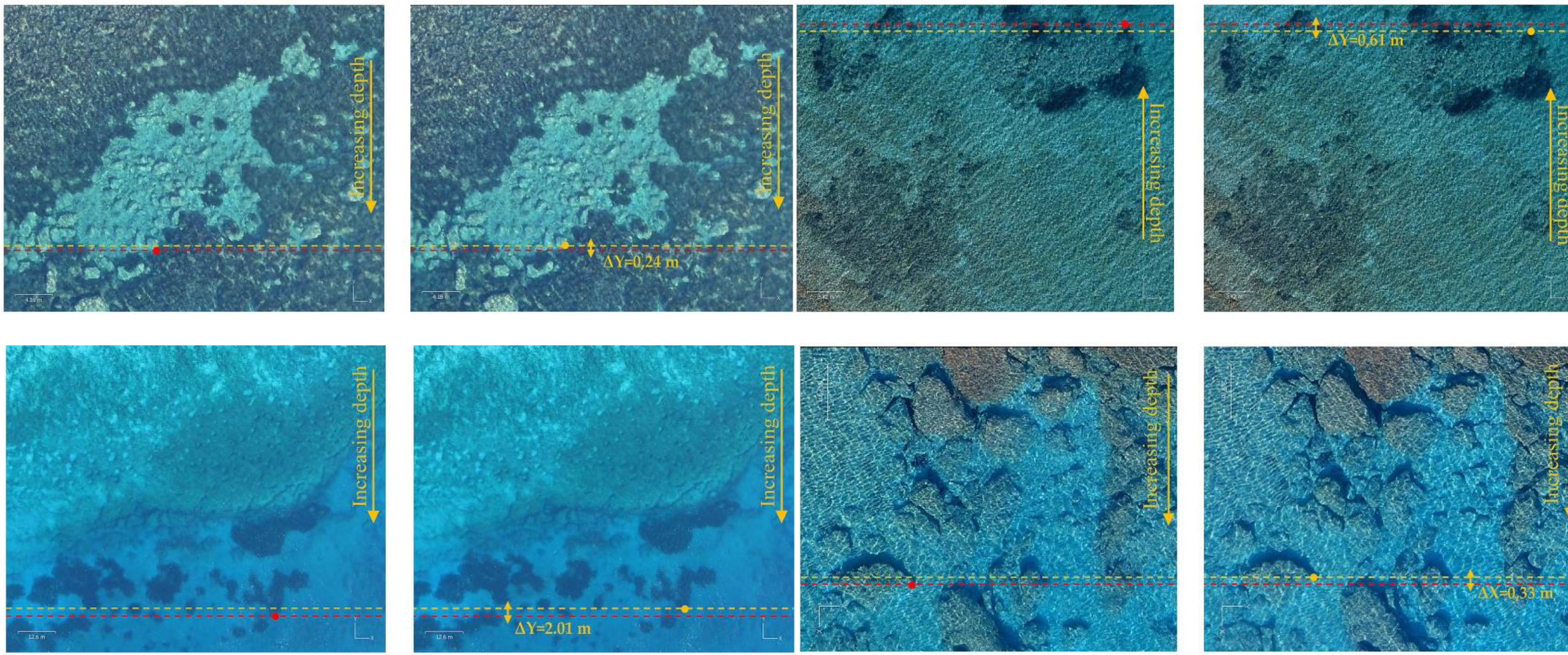

Horizontal error in depth direction reaching 0.182m-0.291m at 1.6m depth and 1.78m-2.07m at 13.8m depth!

Figures: Agrafiotis et al., 2020

Improvements in texture

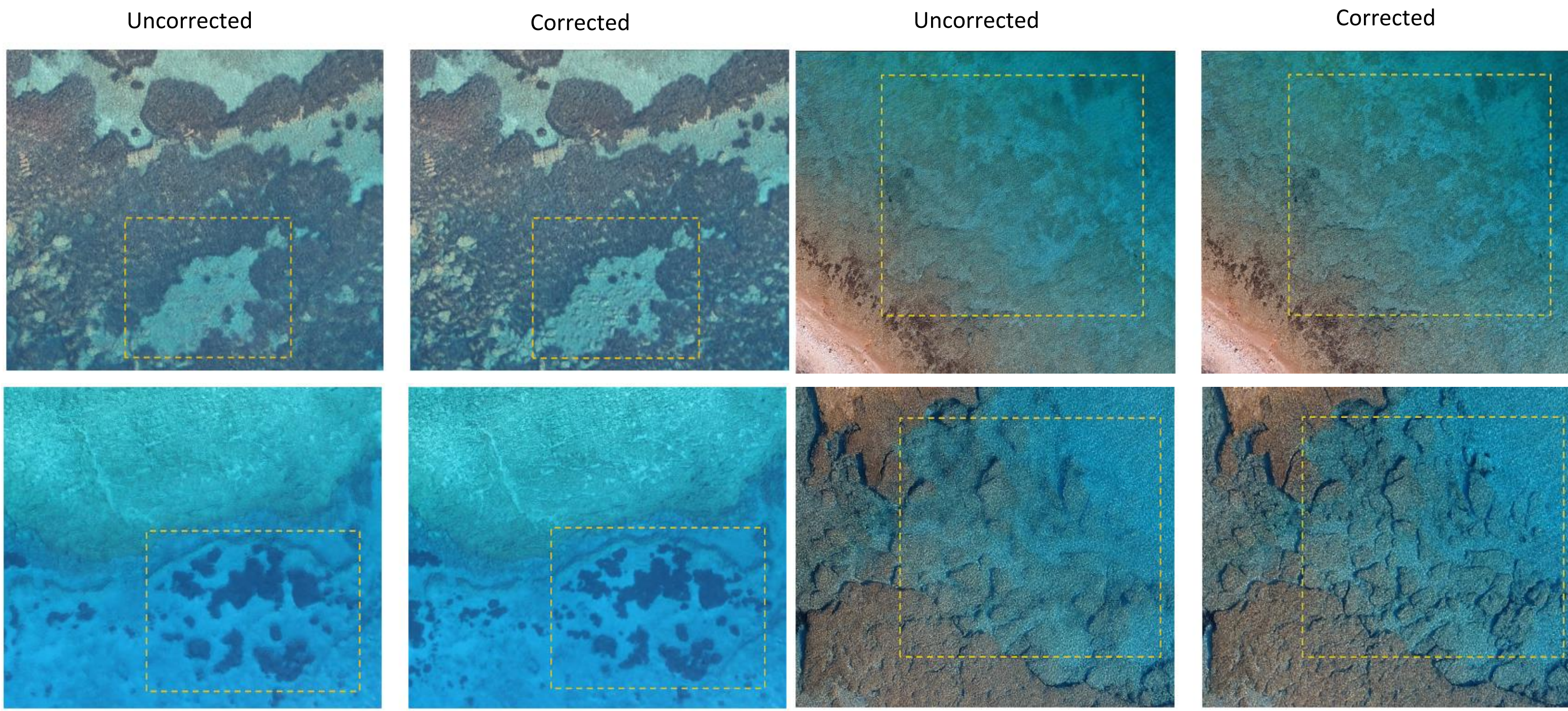

By correcting the images from refraction, the texture of the 3D model is improved

Figures: Agrafiotis et al., 2020

Key-point matching difficulties

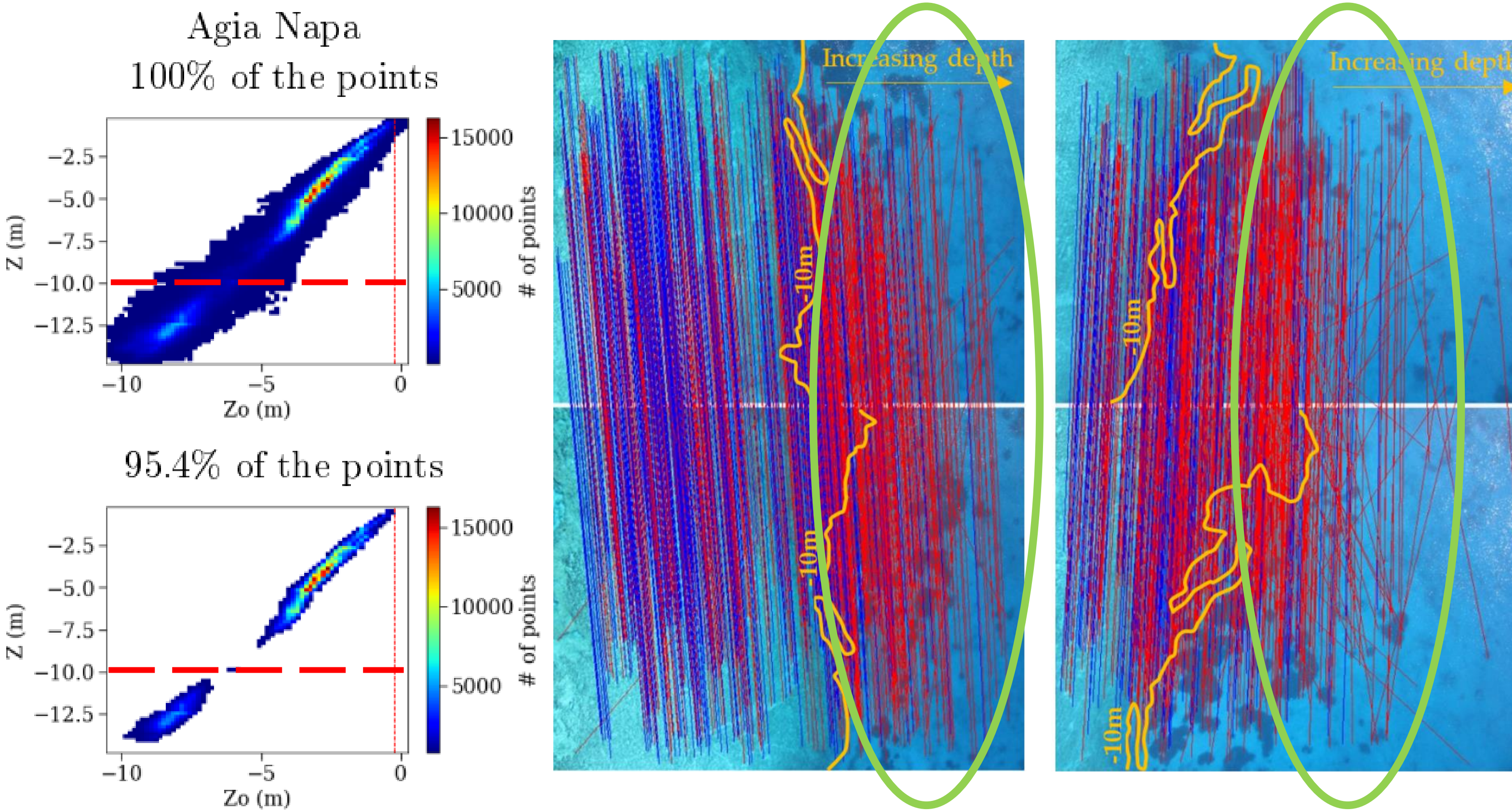

Figures: Agrafiotis, 2020

Bathymetry via active and passive airborne remote sensing

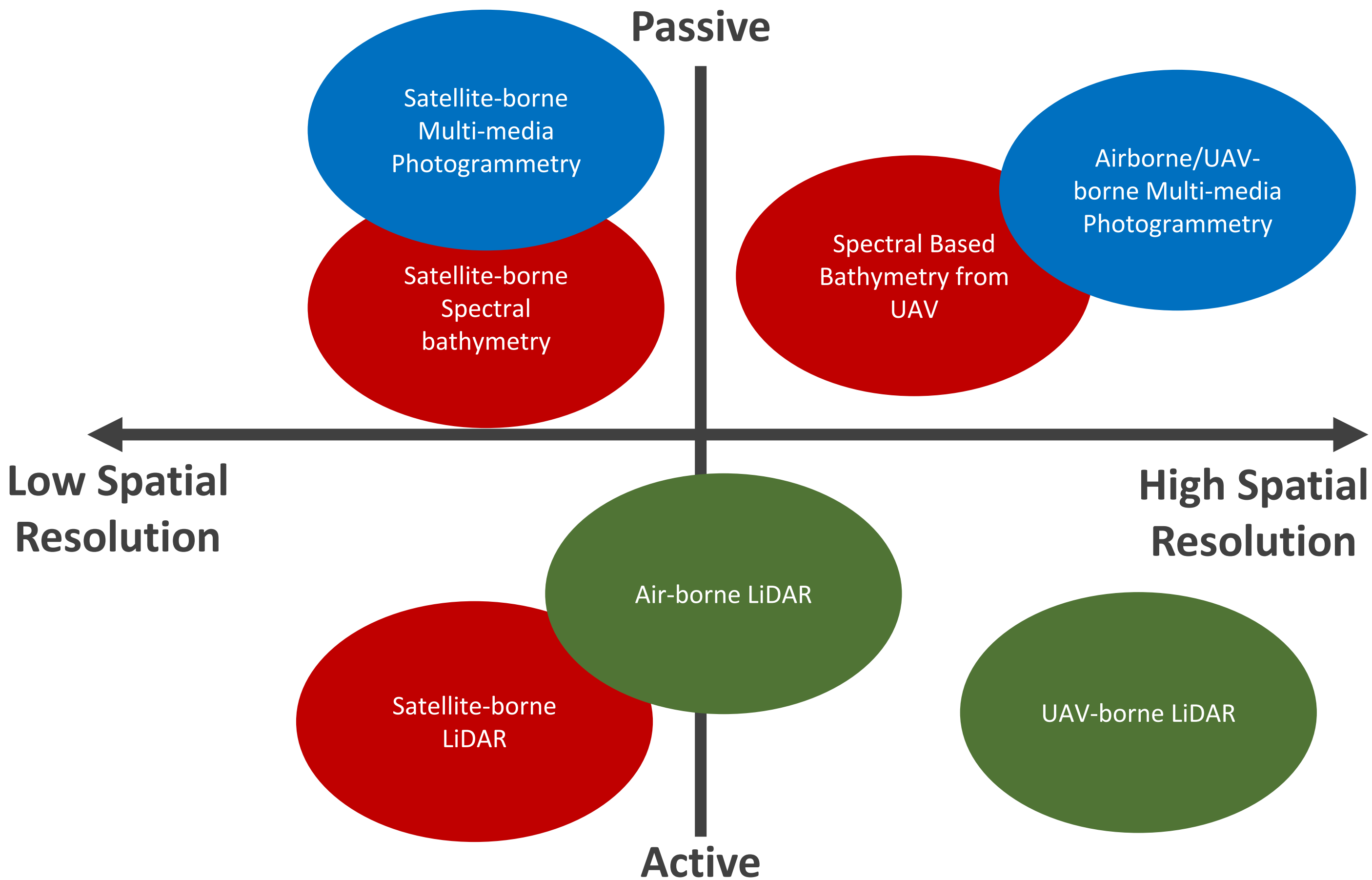

Agrafiotis: Bathymetry from active and passive UAV-borne, airborne and satellite-borne remote sensing

Wrap up

Airborne Laser Bathymetry – refraction correction is necessary!

- Active method
- Geometric & radiometric (intensity)
- Measures the depth via round trip time measurement & Delivers bottom reflectance
- Independent from external illumination and availability of texture
- Spatial resolution limited by relatively large laser footprint (~50 cm)
- Max depth ~ 3 Secchi

Multi-media photogrammetry - refraction correction is necessary!

- Passive method
- Geometric
- Requires texture to perform SfM-MVS
- Measured depth through triangulation & Delivers colour information
- Delivers high point density in shallow water areas
- Max depth ~ 1 Secchi

ALL the geometric methods need refraction correction!!!

Spectrally based bathymetry

- No sophisticated geometry processing necessary
- Requires visibility of bottom features (similar to SfM-MVS, but not texture is required here)
- Can handle certain differences in substrate type and water clarity
- Requires ground-truth for calibrating coefficients
- Covers large areas (satellite)
- Max depth ~ 1 Secchi

Agrafiotis: Bathymetry from active and passive UAV-borne, airborne and satellite-borne remote sensing

References

1. Agrafiotis, P. G. (2020). Image-based bathymetry mapping for shallow waters., PhD Thesis, National Technical University of Athens
2. Agrafiotis, P., Karantzalos, K., Georgopoulos, A., & Skarlatos, D. (2020). Correcting image refraction: Towards accurate aerial image-based bathymetry mapping in shallow waters. *Remote Sensing*, *12*(2), 322.
3. Agrafiotis, P., Skarlatos, D., Georgopoulos, A., & Karantzalos, K. (2019). DepthLearn: learning to correct the refraction on point clouds derived from aerial imagery for accurate dense shallow water bathymetry based on SVMs-fusion with LiDAR point clouds. *Remote Sensing*, *11*(19), 2225.
4. Bianco, G., Muzzupappa, M., Bruno, F., Garcia, R., & Neumann, L. (2015). A new color correction method for underwater imaging. The International Archives of Photogrammetry, Remote Sensing and Spatial Information Sciences, 40(5), 25.
5. Caballero, I., & Stumpf, R. P. (2020). Towards routine mapping of shallow bathymetry in environments with variable turbidity: contribution of Sentinel-2A/B satellites mission. *Remote Sensing*, *12*(3), 451.
6. Geyman, E. C., & Maloof, A. C. (2019). A simple method for extracting water depth from multispectral satellite imagery in regions of variable bottom type. *Earth and Space Science*, *6*(3), 527-537.
7. Ilori, C. O., & Knudby, A. (2020). An Approach to Minimize Atmospheric Correction Error and Improve Physics-Based Satellite-Derived Bathymetry in a Coastal Environment. *Remote Sensing*, *12*(17), 2752.
8. Legleiter, C. J., Overstreet, B. T., & Kinzel, P. J. (2018). Sampling strategies to improve passive optical remote sensing of river bathymetry. *Remote Sensing*, *10*(6), 935.
9. Lyzenga, D. R. (1978). Passive remote sensing techniques for mapping water depth and bottom features. *Applied optics*, *17*(3), 379-383.
10. Mandlburger, G., Pfennigbauer, M., & Pfeifer, N. (2013). Analyzing near water surface penetration in laser bathymetry—A case study at the River Pielach. *ISPRS Annals of the Photogrammetry, Remote Sensing and Spatial Information Sciences*, *5*, W2.
11. Parrish, C. E., Magruder, L. A., Neuenschwander, A. L., Forfinski-Sarkozi, N., Alonzo, M., & Jasinski, M. (2019). Validation of ICESat-2 ATLAS bathymetry and analysis of ATLAS's bathymetric mapping performance. Remote sensing, 11(14), 1634.
12. Stumpf, R. P., Holderied, K., & Sinclair, M. (2003). Determination of water depth with high-resolution satellite imagery over variable bottom types. *Limnology and Oceanography*, *48*(1part2), 547-556.